Available online at www.sciencedirect.com
ScienceDirect
Cement and Concrete Research 37 (2007) 310–318
Cement and Concrete Research

Probing the microstructure and water phases in composite cement blends

Jean-Philippe Gorce *, Neil B. Milestone

Immobilisation Science Laboratory, Department of Engineering Materials, University of Sheffield, Sheffield S1 3JD, UK

Received 1 October 2005; accepted 18 October 2006

Abstract

^{1}H nuclear magnetic resonance relaxometry has been used in combination with the more conventional techniques of mercury intrusion porosimetry, freeze-drying and thermogravimetric analysis to investigate the evolution of the microstructure and the distribution of water phases in two composite cement blends hydrating over a one year period. These two blends are composed of high substitution of Ordinary Portland Cement (OPC) with Blast Furnace Slag (BFS) at level of 75 wt.% (3:1 blend) and 90 wt.% (9:1 blend).

After one year, the 3:1 blend microstructure is characterised by poorly interconnected gel pores filled with about 35 vol.% of water while less than 4 vol.% of water is trapped in remaining capillary pores. The 9:1 blend microstructure is characterised by a network of larger gel and capillary pores filled with about 21 and 22 vol.% of water respectively. Further hydration is ruled out for this blend.

Keywords: NMR; (B) Pore size distribution; (B) Mercury porosimetry; (D) Blended cement; (E) Radioactive waste

1. Introduction

Cementitious materials are used in existing and planned multi-barrier underground facilities designed for the long term disposal of nuclear wastes resulting from the activity of the nuclear energy industry. In the United Kingdom, Low and Intermediate Level radioactive Wastes (LLW and ILW) account for more than 95% of the total volume of conditioned wastes [1]. ILW contain metal swarf from fuel cans, filters and residues from effluent treatments. Their radioactivity level is too low to release significant heat but they contain enough radioactive materials to require special treatment to minimize any potential release into the biosphere [2,3].

Composite cement systems are used worldwide to form solid waste matrices which directly encapsulate and immobilise ILW. These are more easily and more safely managed than the initial waste streams. The relatively low cost, well known processing technology easily transferable to remote handling, the wide applicability for a variety of waste streams, the good radiation stability and ultimate durability, and the capacity to immobilise many radionucleides are the main attributes making composite cement systems suitable for the safe processing of large volume of ILW [4].

Cement blend matrices composed of high substitution of Ordinary Portland Cement (OPC) with Blast Furnace Slag (BFS) are the preferred option in the UK nuclear waste encapsulation plants. ILW and cement blend grouts are mixed in 500 l stainless steel drums which provide an additional barrier to environmental attacks. At this stage, the monoliths (encapsulated wastes within a steel drum) are expected to deliver optimal encapsulation capabilities for interim surface storage for periods which might exceed 100 years. The quality of the encapsulation is essential to achieve the full potential of the wasteform longevity and reduce the risks of re-working or re-packaging monoliths before final disposal in underground repository. Unfortunately, the inspection of the containers left above ground over the years has revealed some signs of mechanical stresses with cracks and fractures observed in some wasteform matrices. In extreme cases, deformation of the stainless steel drums was observed. This development of mechanical stress has been linked to the corrosion of the metals present in the encapsulated wastes (i.e. aluminium and Magnox swarf). The corrosion is driven by the availability of an alkaline pore solution. As the

* Corresponding author.
E-mail addresses: j.gorce@sheffield.ac.uk, j.gorce@lycos.co.uk (J.-P. Gorce).

0008-8846/$ - see front matter © 2006 Published by Elsevier Ltd.
doi:10.1016/j.cemconres.2006.10.007

corrosion products develop, the waste volume increases and stress builds up.

One of the challenges faced by the nuclear industry is to be able to predict the lifetime expectancy of these solid monoliths. This prediction requires a better understanding of the waste corrosion process within a cementitious environment. The presence of water phases in hardening cement matrices is therefore a main issue. The identification and quantification of water phases available for hydration and/or corrosion over the long term are required. Finally, the cement matrix microstructure plays a significant role in facilitating the transport and availability of such aqueous phases towards the corrosion sites, and therefore needs to be characterised over long period of time.

In this paper, the microstructure and the distribution of water phases in two BFS:OPC matrices have been investigated by ^{1}H Nuclear Magnetic Resonance Relaxometry, in conjunction with Mercury Intrusion Porosimetry, thermogravimetric and freeze-drying techniques. The two blends are prepared using OPC substituted with either 75 wt.% or 90 wt.% of BFS. These values are currently the two extreme BFS substitution levels acceptable for the encapsulation of ILW in the UK.

1.1. Cement hydration and water phases

Cement requires water to harden. The main hydration products are an amorphous hydrated calcium silicate of variable composition, usually given the symbol C–S–H, and $Ca(OH)_2$. Theoretically, a water-to-cement weight ratio (w/c) of 0.24 should be sufficient to fully hydrate cement based on the chemically bound water [5] but a w/c ratio of about 0.38 is necessary to obtain full hydration as the hydration reaction is expansive and the C–S–H needs space into which it grows [5–7]. The extra water is held in a series of pores which have been defined empirically [5–7]. These are traditionally presented in decreasing order of ease of removal from the paste as capillary water, interlayer water and chemically bound water. Capillary water is defined as water held in pores with a radius typically larger than 100 nm. Interlayer water, often called gel water, is water held by capillary pressure and strong hydrogen bonding between C–S–H gel layers, typically a few nanometres thick. Finally, chemically bound water is that taking an intrinsic part in the hydrate chemical structures and removable only by thermal degradation of the matrix. It is ions held in the capillary water together with the capillary water itself that are thought to be responsible for internal reactions associated with metal corrosion.

In composite cement systems such as BFS:OPC blends, the situation is more complex and the development of the microstructure and properties of C–S–H are not as well defined. BFS is a latent hydraulic material that reacts very slowly when mixed with water at room temperature. It can be activated with an alkaline solution [8,9]. In BFS:OPC blends, $Ca(OH)_2$ from the hydration of OPC acts as an activator [10,11]. As the BFS fraction increases in a cement blend, the degree of BFS activation is reduced [12]. Because its heat of hydration is considerably lower than that of cement, BFS is used to reduce the overall heat liberated during hydration to avoid cracking due to thermal stresses. This reduction in heat output is the main reason why the waste encapsulation industry use blended cement systems. In addition to reduced heat output, blended systems can improve the immobilisation capabilities of the cement matrix by increasing the proportion of fine pore populations and increasing the matrix resistance to potential chemical attacks from the surroundings [3,4,7,10].

1.2. Techniques

^{1}H Nuclear Magnetic Resonance relaxometry is sensitive to the dynamics and chemical and physical environments of ^{1}H nuclei on water molecules found in porous materials. The parameters measured are the ^{1}H magnetisation relaxation times. Earlier studies have demonstrated the correlation between these relaxation times and the degree of confinement of water molecules in porous media in general (developed from Ref. [13]) and in hydrating cement pastes in particular [14–16]. It is postulated that if water molecules are able to probe fully the pore microstructure during the time scale of an NMR pulse sequence (case of the fast exchange model [13]), then the relaxation times are averages based on the volume fraction of molecules at the solid interfaces and in the bulk liquid. In the simplest scenario, three main modes of relaxation separated by at least an order of magnitude are assigned to water molecules in capillary pores, interlayer water in the C–S–H gel structure and water that is chemicaly combined to the hydrated cement matrix itself [14,17]. In such water phases, the ^{1}H spin–spin relaxation times measured (T_2, rate at which the NMR signal dies away due to dipole interactions between neighbouring nuclei) are typically found to be: above 1 ms, 100 μs and about 10 μs respectively. T_2 values are measured using a Carr–Purcell–Meiboom–Gill (CPMG) pulse sequence [18]. The CPMG signal is a superposition of a series of exponential decays, each decay being characteristic of ^{1}H water molecules relaxing in pores of a particular surface to volume ratio [16,17,19]. Because of the nature of the pore network in the cementitious materials, relaxation time distributions rather than discrete values are expected. Relaxation time distributions are obtained by numerical Laplace inversion of the ^{1}H NMR CPMG signal using the UPEN program developed by Borgia et al [20]. The area under the distributions is proportional to the volume of evaporable water in the matrix. It will be used to estimate the relative volume fraction of water in capillary and C–S–H gel pores only. The chemically bound water is not detected by the CPMG pulse sequence because of the extremely short spin–spin relaxation time associated with ^{1}H on such water molecules. This technique has the advantages that it is non-invasive (there is no need to introduce a molecular dye as ^{1}H from liquid water present within the cement microstructure is used as the active NMR probe), non-destructive and multiple measurements can be undertaken over time on the same specimen.

Mercury Intrusion Porosimetry (MIP) is a technique commonly used for the investigation of the pore structure (porosity and pore size distribution) in materials. Its principle is to immerse a sample in a non-wetting liquid (i.e. mercury) and force the liquid into the pore structure of the material by applying increasing pressure. The size of the intruded cylindrical pore is found to be inversely proportional to the pressure applied. Knowing the mercury intrusion pressure, P, the surface tension of mercury, γ

(taken as 485 dyn cm^{-1}), the contact angle between mercury and the pore wall, θ (estimated at 130°) and the Washburn–Laplace equation (Eq. (1)) then the cylindrical pore diameter, d, can be calculated as

$$d = \frac{4\gamma\cos\theta}{P} \quad (1)$$

When applied to cementitious materials, the technique requires the sample to be fully dried before any measurements. Several drying techniques have been developed but each one has been found to a different degree to affect the microstructure of the sample under investigation [21,22]. Although MIP is routinely used for the study of the pore structure in hardened cementitious materials, questions do arise about its reliability [23]. The technique suffers from assumptions and draw backs [24]. The pores are assumed to be cylindrical, the contact angle at the pore walls through the structure is assumed to be uniform, the pore structure itself is assumed to be unaffected by the mercury intrusion, and all the pores above a threshold size are assumed to be probed. In fact, the maximum applied pressure available is technically limited which means that only pores typically greater than a few nanometres in radius can be probed. Non-cylindrical pores will be identified by the break-through pressure needed for mercury to pass through their throats, while the volume will be proportional to the full pore itself. This causes an overestimation of the population of smaller pores. Finally, in the case of poorly connected pore structures, the applied mercury pressure can be sufficient to break the partitions between non-connected but adjacent pores. The volume created by this break-through pressure will be wrongly assigned to a pore size. There is a greater chance of the occurrence of such behaviour as the applied pressure is increased, leading to overestimation of the smaller pore population.

Two alternative drying techniques were used successively in order to estimate the amounts of water present in the different environments of the hydrating cement blend matrices. The samples were first freeze-dried. Only the most easily available water is extracted by this method, and corresponds predominantly to water in capillaries, although, it has been argued that part of the water trapped in the C–S–H gel structure is also extracted [5,7]. Secondly, thermogravimetric analysis (TGA) was performed on these freeze-dried samples. This provides some indication of the amount of water trapped within the chemical structure of the cement matrices [25].

2. Materials

Two cement blend matrices were prepared using Portland cement (supplied to the British Nuclear Fuels Ltd specification) substituted with 75 wt.% (3:1) and 90 wt.% (9:1) of BFS (supplied to BNFL specification). The chemical compositions of the OPC and BFS materials used are presented in Table 1 together with their fineness and specific gravity.

For both blends, a water-to-solid weight ratio (w/s) of 0.37 was used. This is well within the range of values required for waste encapsulation processes (typically $0.32 < w/s < 0.42$). It is slightly below the theoretical value of 0.38 defined for complete hydration of pure OPC paste, but due to the composition of the blends, the relative w/c is significantly greater than 0.38. The w/c are equal to 1.48 and 3.7 for the 3:1 BFS:OPC blend and 9:1 BFS:OPC blend respectively (see Table 2 for details).

The blends were prepared in about 500 g batches. Dry BFS and OPC powders were thoroughly mixed in plastic bottles. The homogenised powders were then added progressively over a 5 min period into a mixer bowl containing the correct amount of distilled water while mixing at low speed. The paste was then mixed at high speed for a further 5 min before being poured into either 10 mm diameter glass test tubes or 2.5 cm diameter plastic tubes which were vibrated to remove entrapped air before sealing. The tubes were placed horizontally and rotated for more than 12 h at room temperature to minimize bleeding. Several samples and repeats were prepared in this way. The samples were hydrated at 20 °C for up to 360 days.

3. Experimentation

A low frequency (^{1}H resonant frequency of 20 MHz) bench-top permanent magnet spectrometer from Resonance Instruments Ltd was used for this investigation. A CPMG pulse sequence defined by $[90_x-(\tau-180_y-\tau-\text{echo})_n-\text{RD}]_m$ with $n=256$ echoes and a pulse gap of $\tau=25$ μs was used to record a succession of echo trains over time (90_x and 180_y stand for radio-frequency pulses of nominal spin flip angles 90° and 180° (corresponding to 2.6 and 5.2 μs) with relative quadrature phase x and y respectively). Each CPMG signal was averaged over $m=256$ scans and the repetition delay, RD, was chosen such that $250\ \text{ms} \le \text{RD} \le 1\ \text{s}$. The CPMG sequence is used to refocus magnetisation dephasing as a result of local field inhomogeneities due to variations in magnetic susceptibility. The signal is additionally attenuated by water diffusion through pore space field gradients, hence, measurements at the shortest pulse gaps technically available have been made.

The MIP experiments were conducted on a Micromeritics Poresizer 9320. The solvent substitution method was chosen to dry the samples. The material is immersed in acetone (water is replaced by the solvent) followed by drying under vacuum. After drying, typically about 1.5 g of material (5 pieces having similar shape and size) was placed within the penetrometer

Table 1
Chemical composition for OPC and BFS materials

	OPC	BFS
CaO (%)	64.58	42.1
SiO_2 (%)	20.96	34.5
Al_2O_3 (%)	5.24	13.74
Fe_2O_3 (%)	2.61	0.97
MgO (%)	2.09	7.29
SO_3 (%)	2.46	–
K_2O (%)	0.59	0.49
Na_2O (%)	0.28	0.22
Chloride (%)	0.048	0.022
Free lime (%)	1.9	–
Fineness ($m^2\ kg^{-1}$)	352	286
Specific gravity (g/cm^3)	3.16	2.9

Table 2
Initial amount of water used in both 3:1 and 9:1 BFS:OPC blends

	3:1 BFS:OPC	9:1 BFS:OPC
Water to solid weight ratio, w/s	0.37	0.37
Water to cement weight ratio, w/c	1.48	3.7
Water content in weight percent	27	27
Water content in volume percent	52.3	52

chamber for measurements. Once the chamber is filled with mercury, the injecting pressure was increased up to 210 MPa. This corresponds to an equivalent minimum pore access diameter calculated at 5.9 nm based on the Washburn–Laplace equation (Eq. (1)).

The freeze-drying experiments were conducted as follow. Typically a few grams of material (pieces smaller than 5 mm in length) were placed into a glass test tube, weighed and then, immersed in liquid nitrogen (−195 °C) for about 15 min. This process promotes the formation of ice micro-crystals in larger pores which reduces the compressive stress on smaller pores. Then, the frozen samples were evacuated (about 10 Pa) at room temperature for about 20 h in the vicinity of a water trap kept at −40 °C. Water is extracted from the cement samples by sublimation. By weighing the samples again, the amount of water extracted is calculated as a percentage of initial weight.

Once crushed and ground to a powder (passing a 63 μm sieve), thermal gravimetric analysis was performed on the freeze-dried materials. Typically 20 mg was placed in an alumina crucible and heated from room temperature up to 1000 °C using a 10 °C min^{-1} heating rate and under a flow of nitrogen (20 ml min^{-1}). The mass loss detected between 105 °C and 950 °C is ascribed to the amount of chemically bound water present in the samples [26]. The data are normalised to the initial amount of material used for the run and expressed in weight percent (wt.%). Here, using few assumptions (no more water left in the material after TGA, initial water content used for the paste formulation taken as 27 wt.%), the weight losses are expressed in percent of the paste weight as initially formulated, i.e. before freeze drying. The amounts of chemically bound water should provide a good indication of the degree of hydration in the blends although it is not possible to separate the contributions for OPC and BFS.

4. Results and discussions

4.1. Mercury porosimetry

Typical MIP pore size distributions for the 3:1 and 9:1 BFS:OPC blends are presented up to 90 days of hydration in Fig. 1(a) and (b) respectively. The pore radii cover three orders of magnitude ranging from 3000 nm to 3 nm, this last value being the minimum pre radius experimentally accessible with the maximum injection pressure f 210 MPa.

The mean pore radius and porosity extracted from the MIP distributions are presented in Figs. 2 and 3 respectively.

As the pastes mature, the mean pore radius and porosity decrease in line with that expected from hydrating pastes as the initial large pores become filled by the hydration products. From 3 to 90 days, the mean pore radius (see Fig. 2) decreases from 141 to 4.9 nm in the 3:1 blend while it decreases from 270 to 6.7 nm in the 9:1 blend with the pores in the 9:1 blend being generally larger. This is expected, at least in the short term, as that blend has the highest level of OPC substitution, decreasing the BFS activation. For both blends, a major decrease in average pore size occurs between 3 and 7 days and is ascribed to the loss of the larger capillary pores due to the development of the C–S–H gel around the cement grains. Surprisingly at this stage, the mean pore radius is slightly greater in the 3:1 blend (15 nm compared to 13.7 nm in the 9:1 blend) while after 14 days, the mean radii are similar in both blends. As C–S–H gel growth occurs between the grains, it generates an increasingly poorly interconnected pore network which becomes increasingly difficult to probe using MIP.

It is easy to differentiate the two blends based on their measured porosity (see Fig. 3). The 9:1 blend exhibits significant greater porosity at all ages decreasing from 43 to 30% with time while in the 3:1 blend porosity decreases from 36 to 18%. Even if the blends have similar average mean pore radii, the populations of pores are greater in the 9:1 blend. The difference in the blends porosity is accentuated as hydration time increases. In a previous study, greater porosity and larger BFS particles free of any significant hydration rings were observed by Scanning Electron Microscopy in a 9:1 blend after 90 days compared to a 3:1 blend [27].

From these observations, several comments related to the effect of the level of cement substitution on the microstructure can be drawn. At most hydration times, the MIP pore radii distributions are wider for the 9:1 blend and larger pores are detected.

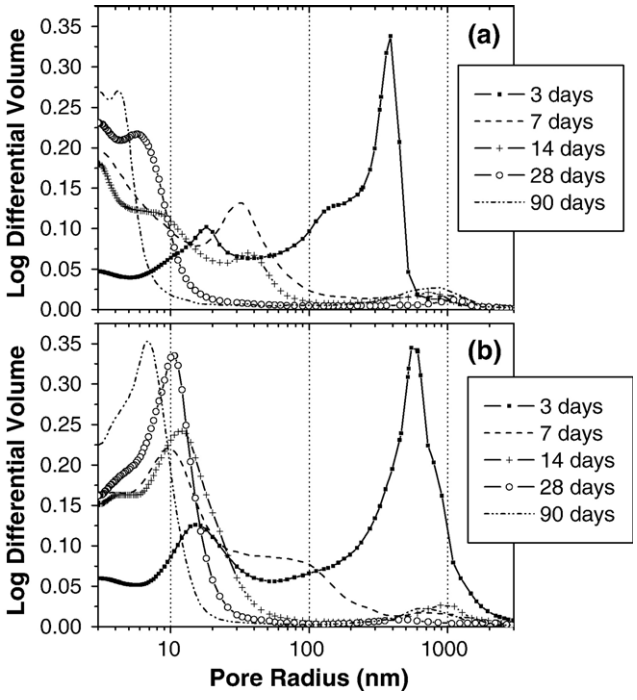

Fig. 1. MIP pore size distributions obtained for (a) 3:1 BFS:OPC blend and (b) 9:1 BFS:OPC blend as a function of hydration time. Vertical dashed lines are major grid lines and a guide to the eye.

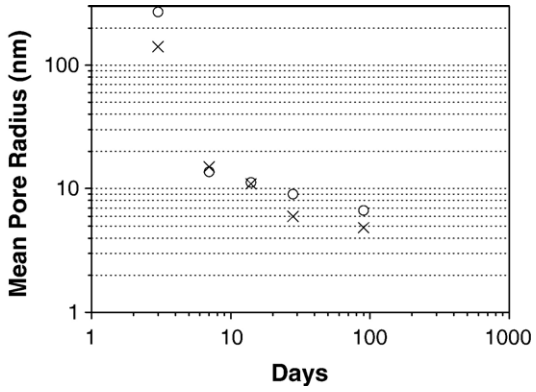

Fig. 2. Mean pore radius estimated by MIP in a 3:1 BFS:OPC blend (crosses) and a 9:1 BFS:OPC blend (open circles) hydrated for 3, 7, 4, 28 and 90 days.

The total porosity (i.e. area under the distributions) is also greater at all times for this blend. This is expected, since at the higher level of OPC substitution, the rate and degree of hydration are expected to be lower, leaving larger amount of capillaries with a reduced amount of gel pores. Consequently, the relative proportion of smaller gel pores is expected to be greater in the 3:1 blend. This is supported by the proportionally large amplitude of pore radii centred at 3 nm which increases over time for the 3:1 blend. These pores having radii of few nanometres are likely to be part of the C–S–H gel layer structure which develops within a restricted space typical of the environment found at the later stage of hydration. MIP is limited in its ability to investigate this part of the microstructure. Thus, the porosity values extracted from the distributions might significantly underestimate the effective porosity in both blends. This might particularly affect the MIP results obtained for the 3:1 blend.

As described earlier, the unexpectedly smaller mean pore radii for the 9:1 blend coupled with the narrowing of the distribution occurring at 7 days might be an indication that an increasingly poorly connected pore network develops and becomes more difficult to probe using MIP. At this stage, the applied mercury pressure might be sufficient to break some of the partitions between non-connected pores. Equally, it could be due to the necking effect. In this respect, the broad population centred about 10 nm present in the 9:1 blend from 7 days onwards might be representative of the applied pressure necessary for mercury to intrude into narrow pore throats or to break thin walls between adjacent pores. The 9:1 blend might be more prone to damage as the mechanical strength of the developing matrix is believed to be lower.

In both blends, small populations of pores found at around 1000 nm and present in some of the later distributions are believed to be due to cracks or fractures which might have developed during the drying process or alternatively during the intrusion of mercury in delicate part of the blend microstructure.

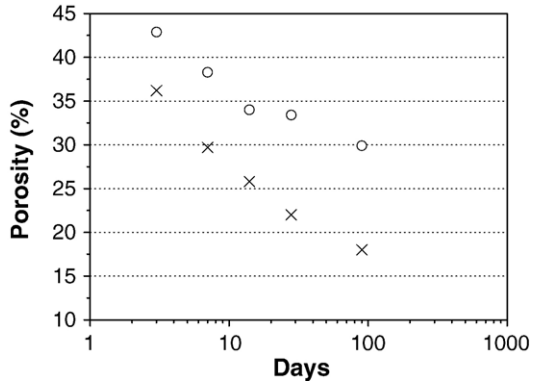

Fig. 3. Porosity estimated by MIP in a 3:1 BFS:OPC blend (crosses) and a 9:1 BFS:OPC blend (open circles) hydrated for 3, 7, 4, 28 and 90 days.

4.2. NMR relaxometry

A selection of NMR relaxation time distributions recorded over up to 360 days are presented in Fig. 4(a) and (b) for both the 3:1 and 9:1 BFS:OPC blends respectively. For both blends, the area under the T_2 distributions recorded after 1 day has been used to normalise the later results.

The major features of the T_2 distributions are presented below, first for the 3:1 blend and then for the 9:1 blend.

For the 3:1 blend (see Fig. 4(a)), the T_2 distribution is continuous and spreads over two orders of magnitude after 1 day. A large amplitude observed above 1 ms is assigned to water in large capillary pores while a lower plateau below 1 ms is ascribed to water molecules in the more constrained environments of the smaller gel pores. At this stage, there is no discrete population of large capillary pores as a significant amount of C–S–H gel has already filled much of the space between the cement grains. After 3 days, the large capillary pores initially present have disappeared as the C–S–H gel builds up. The T_2 distribution becomes

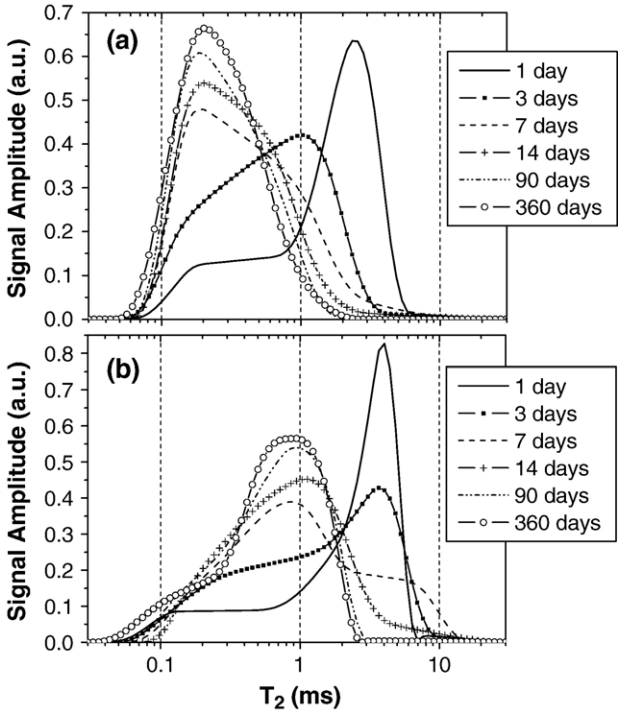

Fig. 4. T_2 relaxation time distributions for (a) 3:1 BFS:OPC blend and (b) 9:1 BFS:OPC blend as a function of hydration time. Vertical dashed lines are major grid lines and a guide to the eye.

narrower spreading over less than two orders of magnitude and shifts towards smaller T_2 values with the largest T_2 population now centred about 1 ms. After 7 days, the distribution width changes with the main pore population shifting to about 0.20 ms. Water molecules are now predominantly found in the small C–S–H gel structures. From 14 days onwards, the 3:1 blend microstructure changes little. The distribution does narrow slightly, spreading over less than two orders of magnitude while there is a further increase in the T_2 population centred about 0.20 ms.

For the 9:1 blend (see Fig. 4(b)), a narrow peak assigned to large capillaries is centred about 4 ms after 1 day. The relative amplitude of this peak is greater than that observed for the 3:1 blend and it occurs at a longer relaxation time. This is not surprising. The greater fraction of BFS present is expected to initially cause a reduction in the amount of the hydration products formed, leaving greater amount of water in larger capillaries. The width of this distribution spreads over 2 orders of magnitude and is greater than that for the 3:1 blend. After 3 days, the large population of large capillaries centred about 4 ms is still the main feature of the microstructure, although the plateau at lower T_2 has levelled off indicating that some C–S–H gel has formed. The distribution still spreads over more than two orders of magnitude. Clearly, hydration is slower and not as efficient at reducing the space between cement grains in this blend. After 7 days, the large capillary pores are no longer predominant. Water molecules become increasingly restricted to smaller developing pores as indicated by the increase of population centred about 0.9 ms. It is interesting to notice that the T_2 population about 0.2 ms has not changed. After 14 days, most of the initial capillary pores centred about 4 ms have vanished, although the distribution is still as wide as it was after 1 day. This is in strong contrast to the results obtained by MIP which show that the pore size distribution was half its initial width at this stage. The size of the population around 0.9 ms increases further. After 90 days, the large capillary pores are lost as the distribution finally narrows, spreading over less than two orders of magnitude with a significant increase in the population around 0.9 ms which is the main feature of the distribution. Little further evolution is observed between 90 and 360 days apart from a slight increase of the populations centred about 0.9 ms and 0.1 ms.

Over the period investigated, the widths of the T_2 distributions are greater for the 9:1 blend, consistently spreading over more than two orders of magnitude in the first 14 days. This is essentially due to the retention of the large capillary pore population centred about 4 ms. On the other hand, for the 3:1 blend, the distribution width becomes increasingly narrower as hydration progresses, with a population of small C–S–H gel pores building about 0.2 ms. For the 9:1 blend, pores with a radius intermediate to the typical capillary and C–S–H gel pores (i.e. centred about 0.9 ms) develop at the later stage of hydration. The differences observed in the evolution of the width of the distributions suggest that both the hydration and pore structure development are affected by the blend composition. In the 3:1 blend, hydration occurs homogeneously throughout the blend microstructure, causing an overall reduction in capillary pore size as a result of C–S–H gel filling the space between particles. This results in the reduction in both the width and amplitude of the distributions above 1 ms. In the 9:1 blend on the other hand, cement hydration occurs more sparsely throughout the blend microstructure leaving some of the original large capillary pores unaffected for up to 14 days. Hence, a population centred about 4 ms is persistently observed although its amplitude decreases during that time. This is supported by a previous study based on the analysis of backscattered electron images suggesting that more localised hydration occurs in a 9:1 blend [27].

Comments on the distributions obtained by MIP and NMR are presented below. The early T_2 distributions are slightly narrower than those obtained by MIP (typically about two against three orders of magnitude). The narrower T_2 distributions could be explained if the large capillary pores were only partially filled with water or were empty. This is unlikely as the large capillary pores initially detected by MIP (and NMR) do disappear as hydration progresses, suggesting that there was initially sufficient water present to allow the on-going build up of C–S–H gel in their core. A more fundamental reason for this discrepancy is more likely to be related to the way the two techniques make their measurements and highlights the well known draw backs of MIP. This is particularly noticeable when the two results for the 9:1 blend are compared. The T_2 distributions retain the same width over the first 14 days of hydration whereas with MIP the width of the distribution is halved suggesting a narrower spread of pores. This could be explained if the sparse inhomogeneous hydration that occurs in the 9:1 blend has created a series of weak barriers which may be broken with the pressure needed for the MIP measurements or which could block access to the larger pores, hence overestimating the fine porosity.

A weighted arithmetic mean for each relaxation time distribution was calculated for both blends and is presented in Fig. 5. Based on the fast exchange model [13] and using several assumptions related to the morphology of the pores (spherical pores fully filled with water) and the relaxation rate of ^{1}H on water molecules at the pore walls (chosen equal to 17 μs, although it is strictly unknown) an estimated mean NMR pore radius can be tentatively assigned to each T_2 value and this is defined on the right hand side y-axis of Fig. 5. As an example,

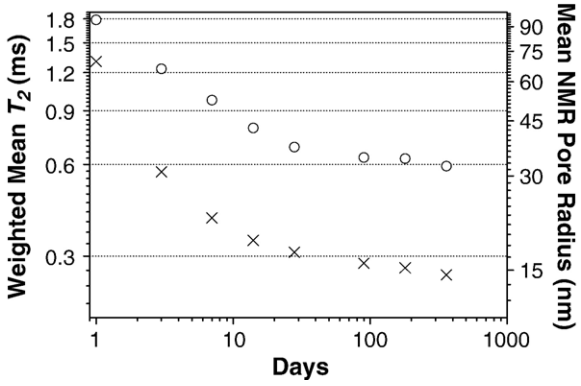

Fig. 5. Mean weighted T_2 for a 3:1 BFS:OPC blend (crosses) and a 9:1 BFS:OPC blend (open circles) as a function of hydration time (the right hand side axis indicates an estimated NMR pore radius).

the T_2 values of 1.3 and 0.26 ms obtained for the 3:1 blend after 1 and 360 days of hydration correspond to an estimated mean NMR pore radius of 69 and 13.8 nm respectively.

The mean T_2 values calculated decrease over time as the available space between cement grains is reduced. At all times, the mean T_2 values are smaller in the 3:1 blend indicating the presence of smaller pores due to a greater level of hydration in this matrix. After about 14 days, the rate at which the T_2 values decrease slows for the 3:1 blend but is still perceptible over the 360 days investigated. A slower rate is observed during the first 28 days for the 9:1 blend, and little variations occur after that time. It is commonly assumed that with a greater BFS content, continued hydration occurs but on a longer time frame. From the results here, it is difficult to see that the 9:1 blend evolves significantly towards a greater degree of hydration after 28 days. This is supportive of a previous study which showed that little, if any, $Ca(OH)_2$ was found by X-ray diffraction in such a blend after about 90 days suggesting a possible end to any further hydration at this stage [27].

The areas under the relaxation time distributions to the right and left of a zone centred about 0.7±0.1 ms have been used to quantify the relative amounts of water in capillaries and gel pores. The choice of this value used for the identification of capillary and gel water may appear subjective but it is based on the observations made on a series of samples. This value corresponds to the end of the plateau observed for the 1 day old distributions and the beginning of the rise of the large population of T_2 assigned to capillary water. The weighted arithmetic means for both capillary and gel water are also estimated following the same procedure.

The results are presented in Fig. 6(a) and (b) for the 3:1 and 9:1 BFS:OPC blends respectively where the relative amounts of each water phase proportional to the diameters of the circles are shown.

In both blends, greater amounts of water are contained in the C–S–H gel structure as hydration progresses. After 3 days, water is predominantly found in small gel pores in the 3:1 blend. After 90 days, more than 90% of the water is found in gel pores. For the 9:1 blend, water is found predominantly in large capillary pores during the first 7 days with increasing amounts of water detected in gel pores as hydration progresses. After 28 days, water is found in similar proportions in gel pores and capillaries.

For the 3:1 blend, the mean T_2 values assigned to gel water decrease over the 360 days period investigated from about 0.29 to 0.23 ms while the values ascribed to capillary water decrease only up to 28 days from about 2.1 to 1.1 ms. After 28 days, the proportion of capillary water is so small that it is difficult to extract meaningful information about the size of the pores. Both the capillary and gel pores decrease in size as hydration progresses.

For the 9:1 blend, the mean T_2 ascribed to capillary water decreases during the first 28 days from about 2.9 to 1.4 ms showing that on average, the capillary pore radius decreases. At the same time, the mean T_2 values assigned to gel water surprisingly increase from about 0.24 to 0.35 ms. As hydration progresses, a broad population of pores centred about 0.9 ms develops which causes this apparent increase in gel pore size. After 28 days, the mean pore radii do not change.

4.3. Gravimetric measurements

Freeze-drying and thermal analysis were conducted in order to determine gravimetrically the absolute content of evaporable and chemically bound water respectively after 3, 7, 14, 28, 90 and 224 days (see Fig. 7). Correcting these into volume percent, the evaporable water contents obtained gravimetrically will be used to transform the relative amounts of water determined by NMR into volume percent.

Over the period investigated, the amount of chemically bound water (closed symbols in Fig. 6) is consistently greater in the 3:1 blend. From 3 days onwards, it increases from about 6.3 to 10.2 wt.% in the 3:1 blend but only from 4.2 to 7.2 wt.% in the 9:1 blend. On the other hand, as expected, greater amounts of evaporable water (open symbols in Fig. 6) are detected for the 9:1 blend. From 7 days onwards, these amounts are found to decrease from about 22.5 to 20.4 wt.% for the 9:1 blend and from only 19.6 to 15.1 wt.% for the 3:1 blend. The data recorded after 90 days, provides an indication of the extent of the uncertainties made during such measurements. These results

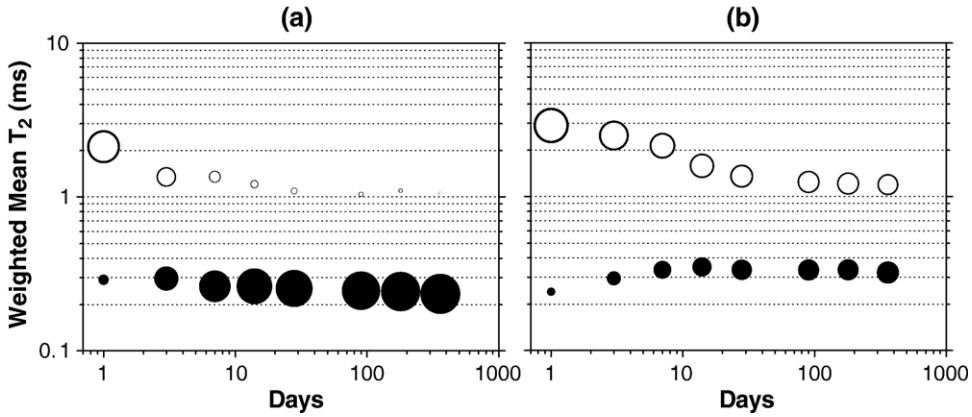

Fig. 6. Weighted mean relaxation time T_2 for ^1H on water molecules in capillaries (open circles) and gel pores (closed circles) as a function of hydration time for (a) 3:1 BFS:OPC blend and (b) 9:1 BFS:OPC blend as a function of hydration time; the diameter of the circles is proportional to the relative content of water in either capillaries or gel.

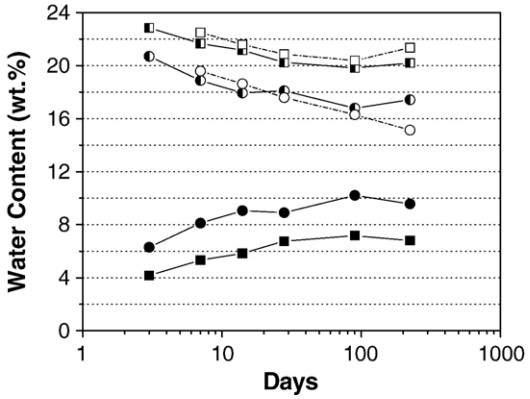

Fig. 7. Chemically bound water content extracted by TGA (fully closed symbols) and evaporable water extracted by freeze-drying (open symbols) in a 3:1 BFS:OPC blend (circles) and in a 9:1 BFS:OPC blend (squares) as a function of hydration time. The semi-open symbols correspond to the amounts of evaporable water deduced from the amount of chemically bound water extracted by TGA.

support the descriptions of the blend matrix made based on the relaxation time distributions. The amounts of evaporable water can also be estimated by subtracting the amounts of chemically bound water determined by TGA from the initial amount of water used to prepare the blends (i.e. 27 wt.%). There is a good agreement between these values and the ones determined directly by freeze-drying. Because these estimated values are consistent and are available over a wider range of hydration times (from 3 days onwards), they have been used to transform the relative water phases contents identified by NMR into volume percent.

The results are presented for the 3:1 and 9:1 blends in Fig. 8 (a) and (b) respectively. The error bars are related to the width of the region used to identify the capillary and gel water phases in the relaxation time distributions (i.e. 0.7 ± 0.1 ms).

For the 3:1 blend (Fig. 8(a)), the amount of gel water increases from about 24 to 35 vol.% between 3 and 180 days. At the same time, the amount of capillary water decreases from about 20 to 4 vol.%. After 180 days, there is a negligible amount of water left in capillary pores, supporting the idea that most of the water has been used for the hydration of this blend. The "hydrated" porosity (total volume of water in capillaries and gel pores as estimated by freeze-drying) varies from about 44 down to 37 vol.% between 3 and 90 days while the porosity estimated by MIP varies from about 36 down to 18 vol.% during the same period. The difference in the porosity values obtained by MIP and freeze-drying is accentuated over hydration time. This is a further confirmation that MIP is increasingly poorly able to probe the pore microstructure as the hydration progresses.

For the 9:1 blend (Fig. 8(b)), the amount of gel water increases from about 15 to 21 vol.% between 3 and 180 days. At the same time, the amount of capillary water decreases from about 32 to 22 vol.%. After 180 days, there is still a very significant amount of water present in large capillaries. The "hydrated" porosity varies from about 47 down to 43 vol.% between 3 and 90 days while the porosity estimated by MIP varies from about 43 down to 30 vol.% during the same period. Although, over time, the difference in the porosity values obtained by MIP and freeze-drying is accentuated, it is not as large as for the 3:1 blend. This is expected as the relative proportion of C–S–H gel is smaller in the 9:1 blend.

5. Conclusion

By using ^{1}H NMR relaxometry in conjunction with more conventional techniques such as MIP, TGA and freeze-drying, the changes in microstructure and water phases in hydrating composite cements can be followed.

In the hydration of a 3:1 BFS:OPC blend, the formation of increasingly smaller gel pores (below a few tens of nanometres) occurs while the larger capillary pores (above 100 nm) disappear quickly. Consequently, both NMR and MIP distributions become narrower. The initial capillary pores found by NMR have T_2 around 2.4 ms, while MIP indicates values of 150 and 400 nm. Developing gel pores can be identified by large population centred about $T_2 = 0.20$ ms and 3–4 nm measured by MIP. After one year of hydration, NMR combined with gravimetric measurements indicate that more than 35 vol.% of water is associated with the gel pores while only 4 vol.% is associated with the capillaries. Hydration is believed to occur homogeneously throughout the microstructure.

For the 9:1 BFS:OPC blend, the capillary pores are larger, measured at 4 ms by NMR and about 600 nm by MIP. These large capillary pores continue to be detected by NMR for the first

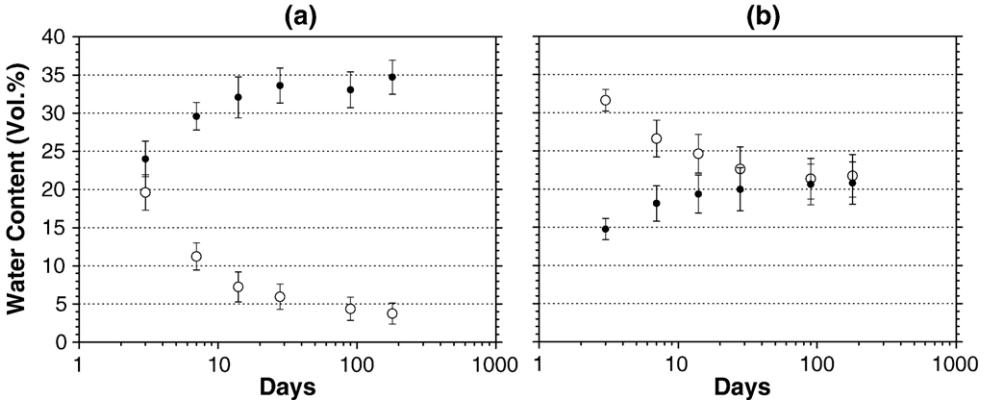

Fig. 8. Absolute water content in capillaries (open circles) and gel pores (closed circles) as a function of hydration time for (a) 3:1 BFS:OPC blend and (b) 9:1 BFS:OPC blend.

14 days of hydration but MIP measurements show an increasingly narrower distribution of pores indicating an inability to detect these larger pores. This suggests that the hydration that occurs is inhomogeneous leaving some of the original large pores intact. Over time, gel pores develop and are centred about 0.9 ms and 7 nm as measured by NMR and MIP. These are larger than those detected for the 3:1 blend. After one year, the water trapped in the gel is only 21 vol.% with 22 vol.% remaining in capillaries.

For the 9:1 blend, the larger amount of water present in larger and perhaps better connected pores might suggest the potential for further hydration in the very long term. However, the lack of changes in the relaxation times distributions observed from 90 days onwards appears to rule out this possibility. Pore water transport will be favoured in this blend so, in presence of encapsulated wastes, the aqueous phases could be made available for metal corrosion.

The 3:1 blend appears to be the matrix of choice if the only concern is to reduce the availability of capillary water for the corrosion of encapsulated metals.

Acknowledgements

We would like to thank Prof. Peter McDonald from the Physics Department of the University of Surrey (UK) for the use of an NMR benchtop as well as for providing guidance and advice on NMR relaxometry. We are grateful to Profs. Robert J. S. Brown and Paola Fantazzini from the University of Bologna for the use of a copy of their UPEN software. We acknowledge more particularly Robert J.S. Brown for his inputs in the investigation of the relaxation times distributions using UPEN. The funding is provided by Nexia Solutions Limited (a British Nuclear Fuel Limited subsidiary company). We would like to thanks Dr. Stephen Farris from Nexia Solutions Limited for his dedication to the project.

References

[1] Radioactive Wastes in the UK — A Summary of the 2001 Inventory, DEFRA/RAS/02.003, Nirex Report N/041, October 2002.
[2] P.D. Wilson (Ed.), The Nuclear Fuel Cycle from Ore to Waste, Oxford Science Publications, 1996.
[3] F.P. Glasser, M. Atkins, Cement in radioactive waste disposal, MRS Bull. 19 (12) (1994) 33–38.
[4] M. Atkins, F.P. Glasser, Application of Portland cement-based materials to radioactive waste immobilisation, Waste Manage. 12 (1992) 105–131.
[5] T.C. Powers, T.L. Brownyard, Studies of the physical properties of hardened Portland cement paste, Bulletin, vol. 22, Research Laboratories of the Portland Cement Association, Chicago, 1948.
[6] A.M. Neville, Properties of Concrete, Pitman Publishing Limited, London, 1981.
[7] H.F.W. Taylor, Cement Chemistry, Academic Press, New York, 1990.
[8] S.-D. Wang, X.-C. Pu, K.L. Scrivener, P.L. Pratt, Alkali-activated slag cement and concrete: a review of properties and problems, Adv. Cem. Res. 7 (27) (1995) 93–102.
[9] A. Fernández-Jiménez, F. Puertas, Alkali-activated slag cements: kinetic studies, Cem. Concr. Res. 27 (3) (1997) 359–368.
[10] I.G. Richardson, C.R. Wilding, M.J. Dickson, The hydration of blastfurnace slag cements, Adv. Cem. Res. 2 (8) (1989) 147–157.
[11] J.I. Escalante-Garcia, J.H. Sharp, Effect of temperature on the hydration of the main clinker phases in Portland cements: part II, blended cements, Cem. Concr. Res. 28 (9) (1998) 1259–1274.
[12] J.I. Escalante, L.Y. Gómez, K.K. Johal, G. Mendoza, H. Mancha, J. Méndez, Reactivity of blast furnace slag in Portland cement blends hydrated under different conditions, Cem. Concr. Res. 31 (2001) 1403–1409.
[13] K.R. Brownstei, C.E. Tarr, Importance of classical diffusion in NMR studies of water in biological cells, Phys. Rev., A 19 (6) (1979) 2446–2453.
[14] L.J. Schreiner, J.C. Mactavish, L. Miljkovic, M.M. Pintar, R. Blinc, G. Lahajnar, D. Lasic, L.W. Reeves, NMR line shape-spin-lattice relaxation correlation study of Portland-cement hydration, J. Am. Ceram. Soc. 68 (1) (1985) 10–16.
[15] L. Miljkovic, D. Lasic, J.C. Mactavish, M.M. Pintar, R. Blinc, G. Lahajnar, NMR studies of hydrating cement: a spin–spin relaxation study of the early hydration stage, Cem. Concr. Res. 18 (6) (1988) 951–956.
[16] W.P. Halperin, J.Y. Jehng, Y.Q. Song, Application of spin–spin relaxation to measurement of surface area and pore size distributions in a hydrating cement paste, Magn. Reson. Imaging 12 (2) (1994) 169–173.
[17] A.J. Bohris, U. Goerke, P.J. McDonald, M. Mulheron, B. Newling, B. Le Page, A broad line NMR and MRI study of water and water transport in Portland cement pastes, Magn. Reson. Imaging 16 (5/6) (1998) 455–461.
[18] S. Meiboom, D. Gill, Modified spin-echo method for measurement of relaxation times, Rev. Sci. Instrum. 29 (1958) 688–691.
[19] P. Boch, A. Plassais, M.-P. Pomies, J.-P. Korb, N. Lequeux, Cementitious nanostructures: nanoporosity, J. Ceram. Process. Res. 5 (2) (2004) 95–100.
[20] G.C. Borgia, R.J.S. Brown, P. Fantazzini, Uniform-penalty inversion of multiexponential decay data II. Data spacing, T_2 data, systematic data errors, and diagnostics, J. Magn. Reson. 147 (2000) 273–285.
[21] C. Gallé, Effect of drying on cement-based materials pore structure as identified by mercury intrusion porosimetry. A comparative study between oven, vacuum and freeze drying, Cem. Concr. Res. 31 (2001) 1467–1477.
[22] L. Konecny, S.J. Naqvi, The effect of different drying techniques on the proof blended cement mortars, Cem. Concr. Res. 23 (1993) 1223–1228.
[23] S. Diamond, Mercury porosimetry. An inappropriate method for the measurements of pore size distributions in cement-based materials, Cem. Concr. Res. 30 (2000) 1517–1525.
[24] R.A. Olson, C.M. Neubaeur, H.M. Jennings, Damage to the pore structure of hardened Portland cement paste by mercury intrusion, J. Am. Ceram. Soc. 80 (9) (1997) 2454–2458.
[24] J.I. Escalante-Garcia, Non evaporable water from neat OPC and replacement materials in composite cements hydrated at different temperatures, Cem. Concr. Res. 33 (2003) 1883–1888.
[26] H.F.W. Taylor, The chemistry and chemically-related properties of cement, in: F.P. Glaser (Ed.), British Ceram. Proc., vol. 35, September 1984, pp. 65–82.
[27] J. Hill, J.H. Sharp, The mineralogy and microstructure of three composite cements with high replacement levels, Cem. Concr. Compos. 24 (2) (2002) 191–199.